Electronic Supplementary Information

# Composite Batteries: A Simple yet Universal Approach to 3D Printable Lithium-Ion Battery Electrodes

Ryan R. Kohlmeyer,[‡*abc] Aaron J. Blake,[‡ad] James O. Hardin,[ac] Eric A. Carmona,[ae] Jennifer Carpena-Núñez,[ab] Benji Maruyama,[a] J. Daniel Berrigan,[a] Hong Huang,[c] and Michael F. Durstock**[a]

[a]*Soft Materials Branch, Materials and Manufacturing Directorate, Air Force Research Laboratory, Wright Patterson Air Force Base, Ohio 45433, USA.*

[b]*National Research Council, Washington, D.C. 20001, USA.*

[c]*UES, Inc., Dayton, Ohio 45432, USA*

[d]*Department of Mechanical and Materials Engineering, Wright State University, Dayton, Ohio 45432, USA*

[e]*Department of Chemical Engineering and Materials Science, University of Minnesota, Minneapolis, Minnesota 55455, USA*

‡ Equal contribution.

*Corresponding author. Tel.: 937-255-9125
**Co-corresponding author. Tel.: 937-255-9159
E-mail address: ryan.kohlmeyer.ctr@us.af.mil (R.R. Kohlmeyer)
michael.durstock@us.af.mil (M.F. Durstock)

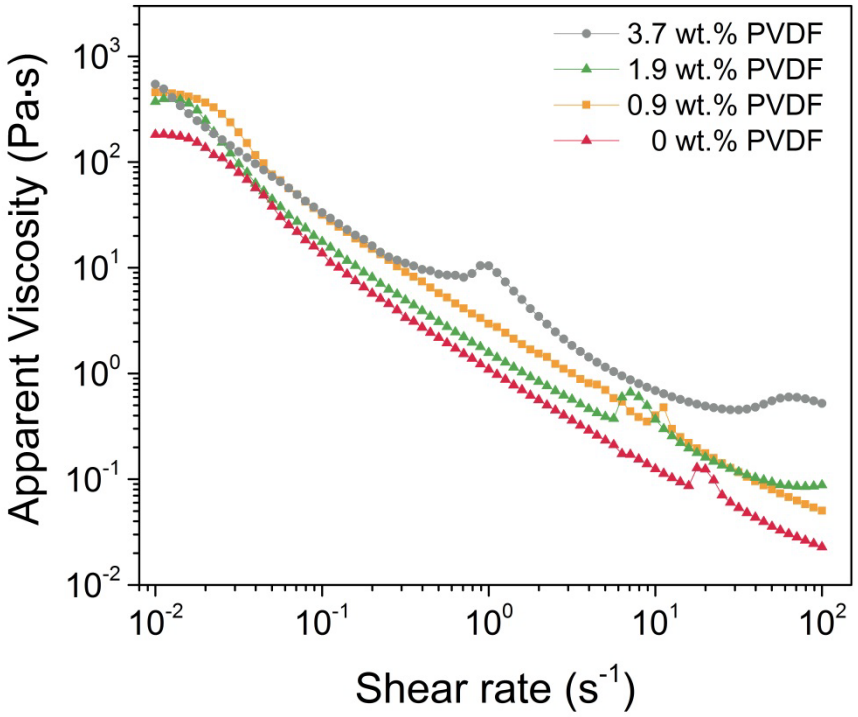


**Fig. S1.** Effect of PVDF loading on shear-thickening behavior of CNF/PVDF solutions in NMP. All samples were prepared in 5 mL of NMP, with a constant CNF loading of 1.9 wt.%.

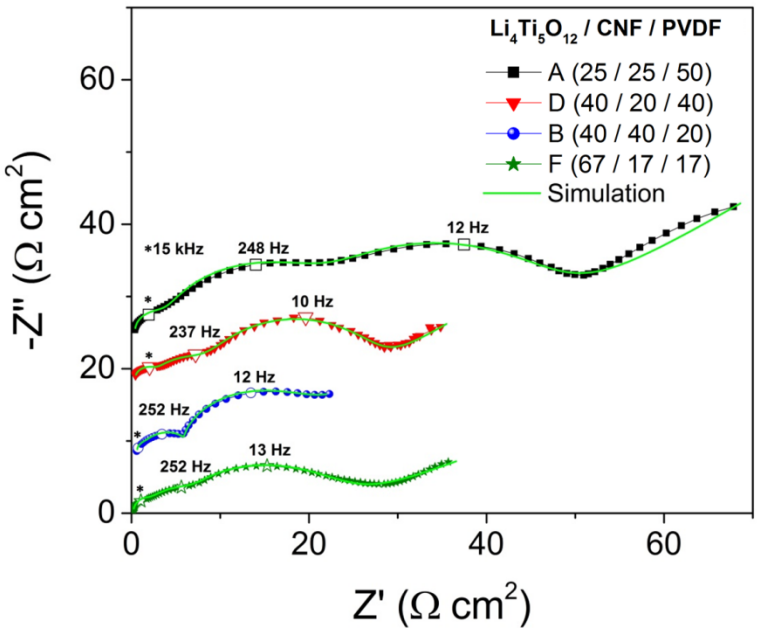


**Fig. S2.** Impedance spectra with model fitting (simulation) of the four $Li_4Ti_5O_{12}$/CNF/PVDF composite electrodes studied in this work. Spectra were shifted along the y-axis for better visual comparison.

**Table S1.** The equivalent circuit parameters obtained from the fit of the experimental impedance spectra. The resistance values have been normalized to areal resistances (A = 1.6 $cm^2$).

| **Set-up** | **3-Electrode** |
|---|---|
| Equivalent circuit | 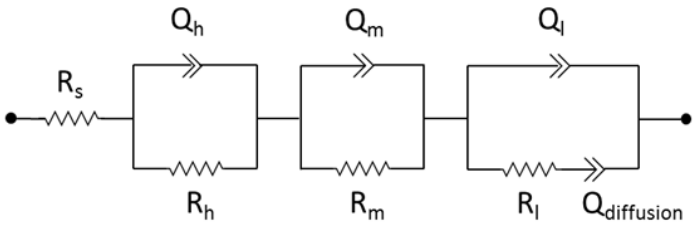 |



| **Component** | **Representation** | **A (25/25/50)** | **D (40/20/40)** | **B (40/40/20)** | **F (67/17/17)** |
|---|---|---|---|---|---|
| $R_s$ (Ω $cm^2$) | Ohmic resistance of liquid electrolyte | 0.41 ± 0.01 | 0.45 ± 0.02 | 0.63 ± 0.02 | 0.24 ± 0.01 |
| $R_h$ (Ω $cm^2$) | Schottky barrier resistance (CNF/LTO interface) | 3.06 ± 0.43 | 2.41 ± 0.37 | 0.99 ± 0.15 | 2.10 ± 0.26 |
| $R_m$ (Ω $cm^2$) | Contact resistance between SS and electrode | 16.67 ± 1.06 | 9.14 ± 1.20 | 5.18 ± 0.58 | 7.84 ± 0.87 |
| $R_l$ (Ω $cm^2$) | Transfer across the phase boundary (spinel/rock-salt) | 18.72 ± 2.79 | 17.79 ± 2.53 | 17.99 ± 2.96 | 18.28 ± 2.66 |

The impedance spectra were fitted to the equivalent circuit shown in Table S1, where the true capacitance has been replaced with a constant phase element (CPE) to better represent the non-homogenous nature of the porous composite electrode. Furthermore, a CPE has replaced the common Warburg element in the above model to more accurately represent the finite diffusion process.

a

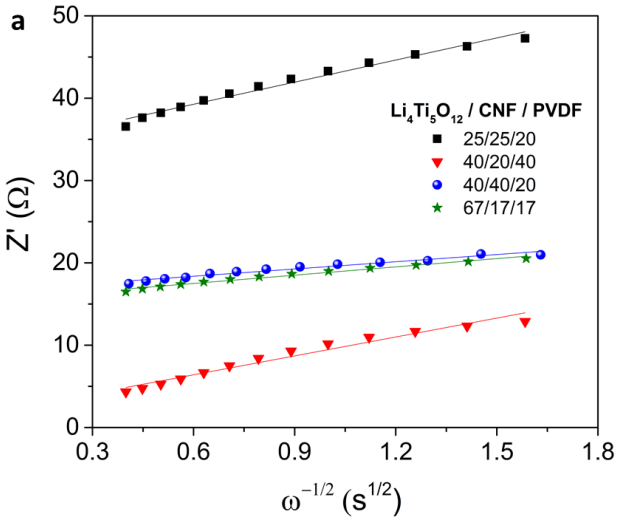


b

| Sample | $A_w$ (Ω $s^{-1/2}$) | $D_{Li^+}$ ($cm^2$ $s^{-1}$) |
|---|---|---|
| A (25/25/50) | 8.95 | 1.5 x $10^{-13}$ |
| D (40/20/40) | 7.65 | 2.0 x $10^{-13}$ |
| B (40/40/20) | 2.93 | 1.4 x $10^{-12}$ |
| F (67/17/17) | 3.35 | 1.1 x $10^{-12}$ |

**Fig. S3**. Determination of $Li^+$ diffusivity via EIS method using Warburg impedance. a) Dependence of the real impedance on frequency for determination of the Warburg coefficient ($A_w$). b) Table of Warburg coefficients and corresponding $Li^+$ diffusivity for each $Li_4Ti_5O_{12}$ composite electrode.

The value of the Warburg coefficient was empirically determined from the slope of the real impedance (Z') versus the reciprocal of the square root of the angular frequency ($\omega^{-1/2}$) (Fig. S3). Because mass transport does not manifest itself as an influencing parameter at high frequency, this portion of the graph could be neglected and only the linear portion at low frequency was analyzed.[1] The parameters $n$ (total number of electrons transferred) and $C$ (molar concentration of lithium) from main text Equation (1) were calculated as follows. The total number of electrons transferred was determined from the electrochemical reaction of spinel lithium titanate:

$$Li_4Ti_5O_{12} + 3Li^+ + 3e^- \leftrightarrow Li_7Ti_5O_{12} \quad \text{(S1)}$$

where we see that the value of total electrons transferred is 3. The molar concentration was obtained from Equation (S2):

$$C = \frac{(x/3)}{459.09\ \text{g mol}^{-1}} \times 3.43\ \text{g cm}^{-3} \quad \text{(S2)}$$

where $x/3$ is the molar ratio of lithium to spinel lithium titanate in $Li_{4+x}Ti_5O_{12}$, 459.09 g $mol^{-1}$ is the molar mass of lithium titanate, and 3.43 g $cm^{-3}$ is the density of lithium titanate. The composition $x$ was taken to be 1.5 (*i.e.*, 50% depth of discharge, DOD), based on the experimental EIS set-up in which the electrode was lithiated to 50% DOD prior to the measurement.

**Table S2.** Parameters describing ionic transport within the composite electrodes: $Li^+$ diffusivity ($D_{Li+}$), mobility ($\mu$), and conductivity ($\sigma_i$).

| Sample | $D_{Li+}$ ($cm^2$ $s^{-1}$) | μ ($cm^2$ $V^{-1}s^{-1}$) | $\sigma_i$ (S $cm^{-1}$) |
|---|---|---|---|
| A (25/25/50) | 1.5 x $10^{-13}$ | 5.9 x $10^{-12}$ | 2.1 x $10^{-9}$ |
| D (40/20/40) | 2.0 x $10^{-13}$ | 8.0 x $10^{-12}$ | 2.9 x $10^{-9}$ |
| B (40/40/20) | 1.4 x $10^{-12}$ | 5.5 x $10^{-11}$ | 2.0 x $10^{-8}$ |
| F (67/17/17) | 1.1 x $10^{-12}$ | 4.2 x $10^{-11}$ | 1.5 x $10^{-8}$ |

In order to fully describe ionic motion and to understand the ease with which ions pass through the electrode under a concentration gradient or external electric field, it was necessary to derive both the mobility and ionic conductivity in addition to the diffusivity. The ionic mobility μ is related to the diffusivity by the Nernst-Einstein equation:

$$\mu = \frac{zeD_{Li^+}}{k_B T} \tag{S4}$$

where $z$ is the ion valence, $e$ is the elementary charge, $k_B$ is the Boltzmann constant, and $T$ is the absolute temperature. The motion of $Li^+$ is then defined by the ionic conductivity, which can be calculated according to

$$\sigma_i = n \cdot z \cdot e \cdot \mu \tag{S3}$$

where n is the molar concentration of lithium ($C$) multiplied by Avagadro's number ($6.022 \times 10^{23}$ atom $mol^{-1}$). Combined with diffusivity, these parameters fully define the ionic transport properties of the electrode material. It was observed that sample B exhibited the highest ionic transport properties compared with the other composites.

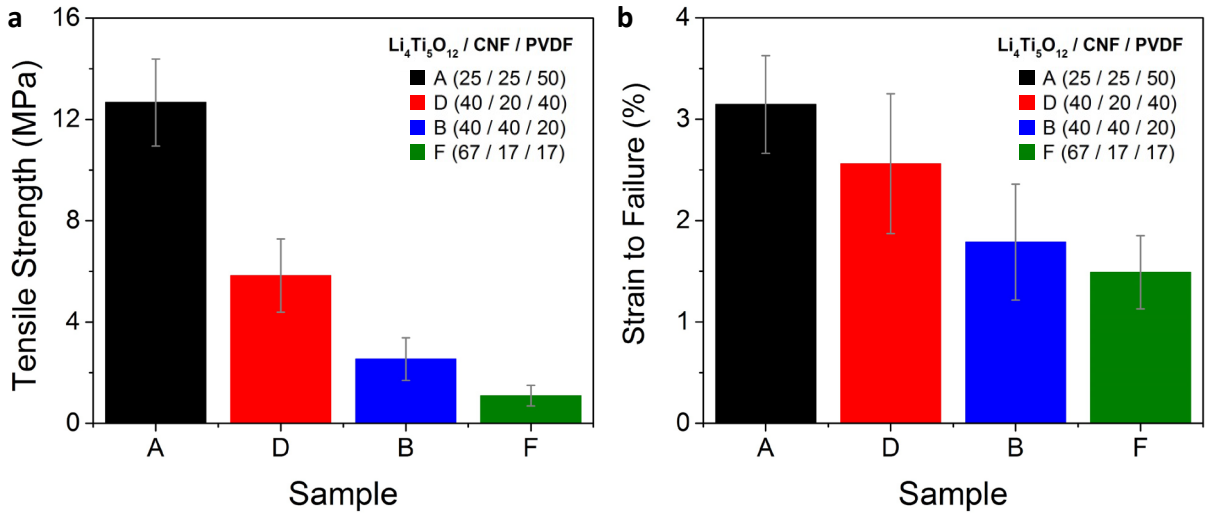


**Fig. S4.** Average mechanical properties of $Li_4Ti_5O_{12}$/CNF/PVDF composites. The mean (a) tensile strength and (b) strain at failure were calculated from five or more samples at each loading. Error bars are included which display the 95% confidence interval for each sample.

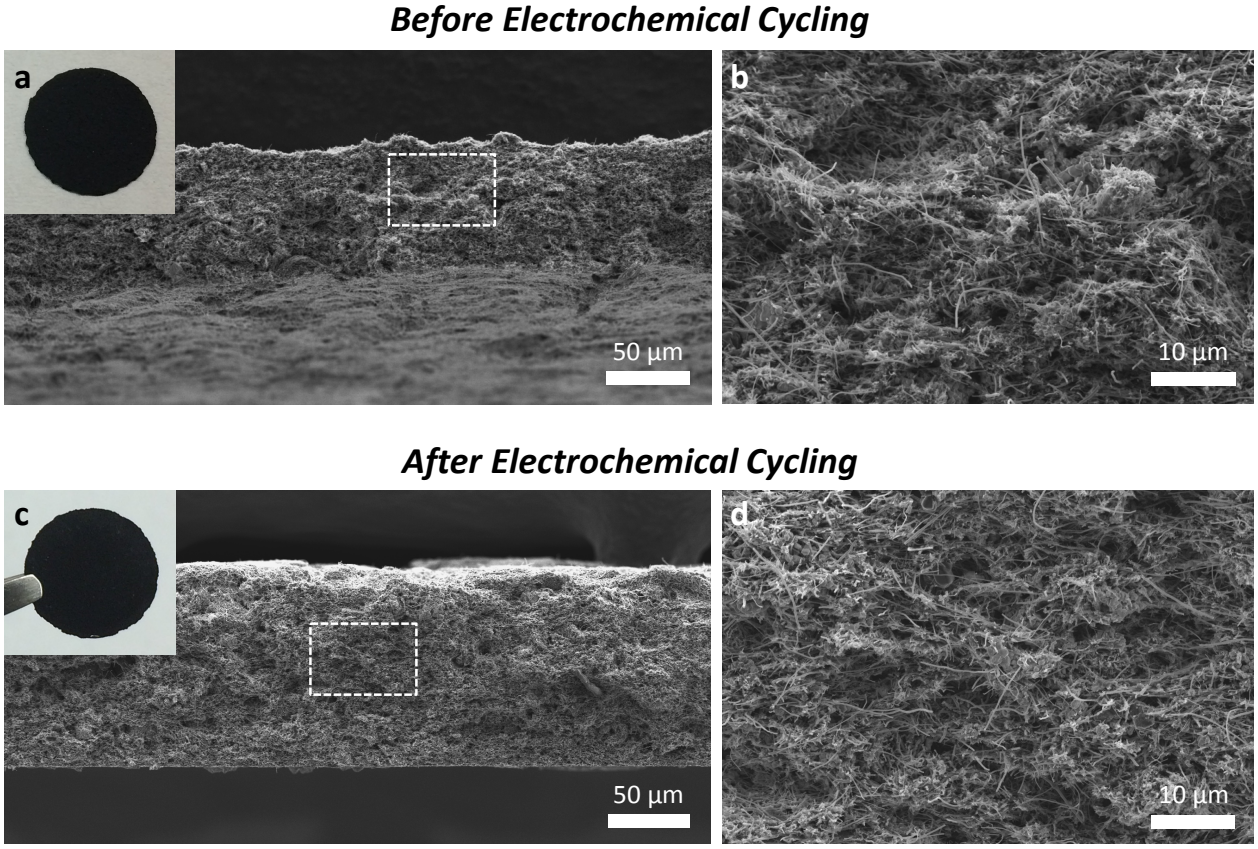


**Fig. S5.** Characterization of sample B before and after electrochemical cycling through a 30 cycle rate performance study as shown in Fig. 2a. (a,b) Cross-sectional SEM images before cycling. The SEM image in (b) was taken at the dashed white box in (a). The inset in (a) is photograph of a 9.5 mm diameter sample B disc before cycling. (c,d) Cross-sectional SEM images after cycling. The SEM image in (d) was taken at the dashed white box in (c). The inset in (c) is photograph of the same 9.5 mm diameter disc from the inset in (a) after cycling.

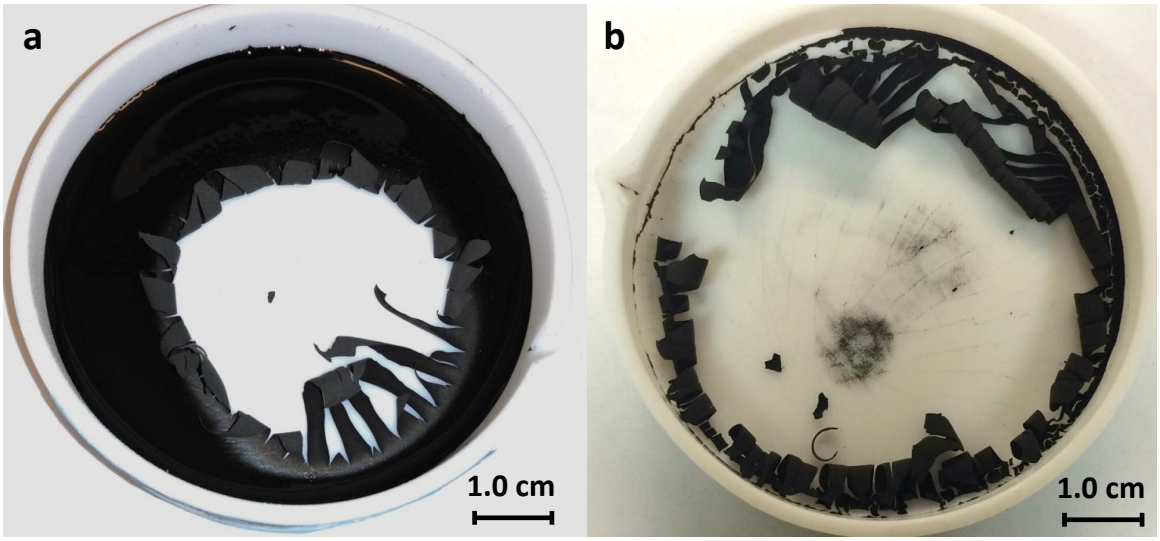


**Fig. S6.** Photographs of a 40/40/20 $Li_4Ti_5O_{12}$/Carbon Black/PVDF composite (sample H). Photographs of the composite (a) after partial drying and (b) after complete drying at 90 °C.

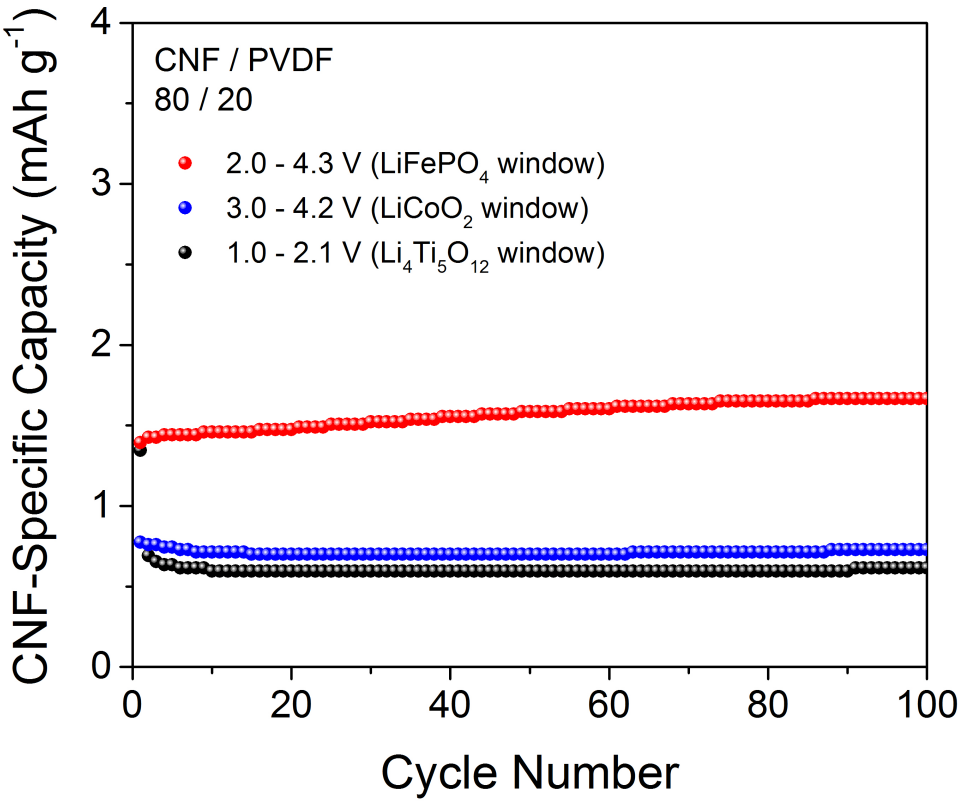


**Fig. S7.** Cycling performances (0.2C) of a CNF/PVDF (80/20) composite cycled at the voltage windows for $LiFePO_4$ (red), $LiCoO_2$ (blue), and $Li_4Ti_5O_{12}$ (black).

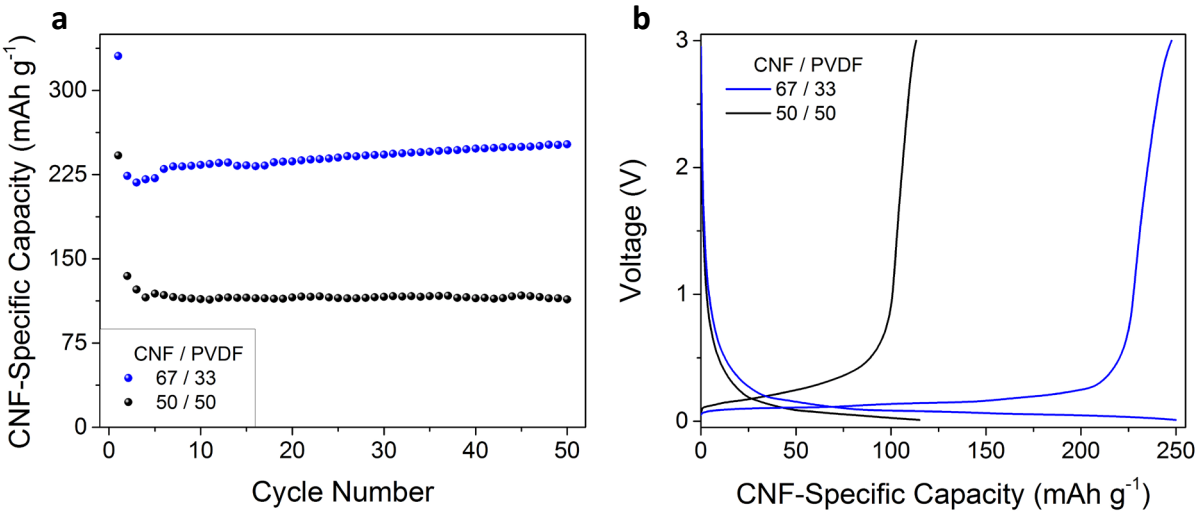


**Fig. S8.** Electrochemical properties of pure CNF/PVDF composites. (a) Cycling performances (0.2C) and (b) representative charge/discharge profiles (0.2C) of 67/33 (sample L, blue) and 50/50 (sample K, black) CNF/PVDF composites.

Composites consisting of only CNFs and PVDF were prepared with CNF/PVDF ratios of 50/50 (sample K) and 67/33 (sample L). Both of these composite ratios formed free-standing, flexible films, but there was a tradeoff between electrochemical performance and mechanical strength. Although both samples showed excellent 0.2C cyclability over 50 cycles, sample K with 50% CNFs was only able to achieve a reversible capacity of 115 mAh $g^{-1}$, whereas sample L with 67% CNFs showed a 250 mAh $g^{-1}$ CNF-specific capacity (Fig. S7). This decreased electrochemical performance can be attributed to increased polymer loading, which fills the voids within the composite, blocking potential diffusion pathways, but leads to a nearly 3 fold enhancement in tensile strength (Table 1).

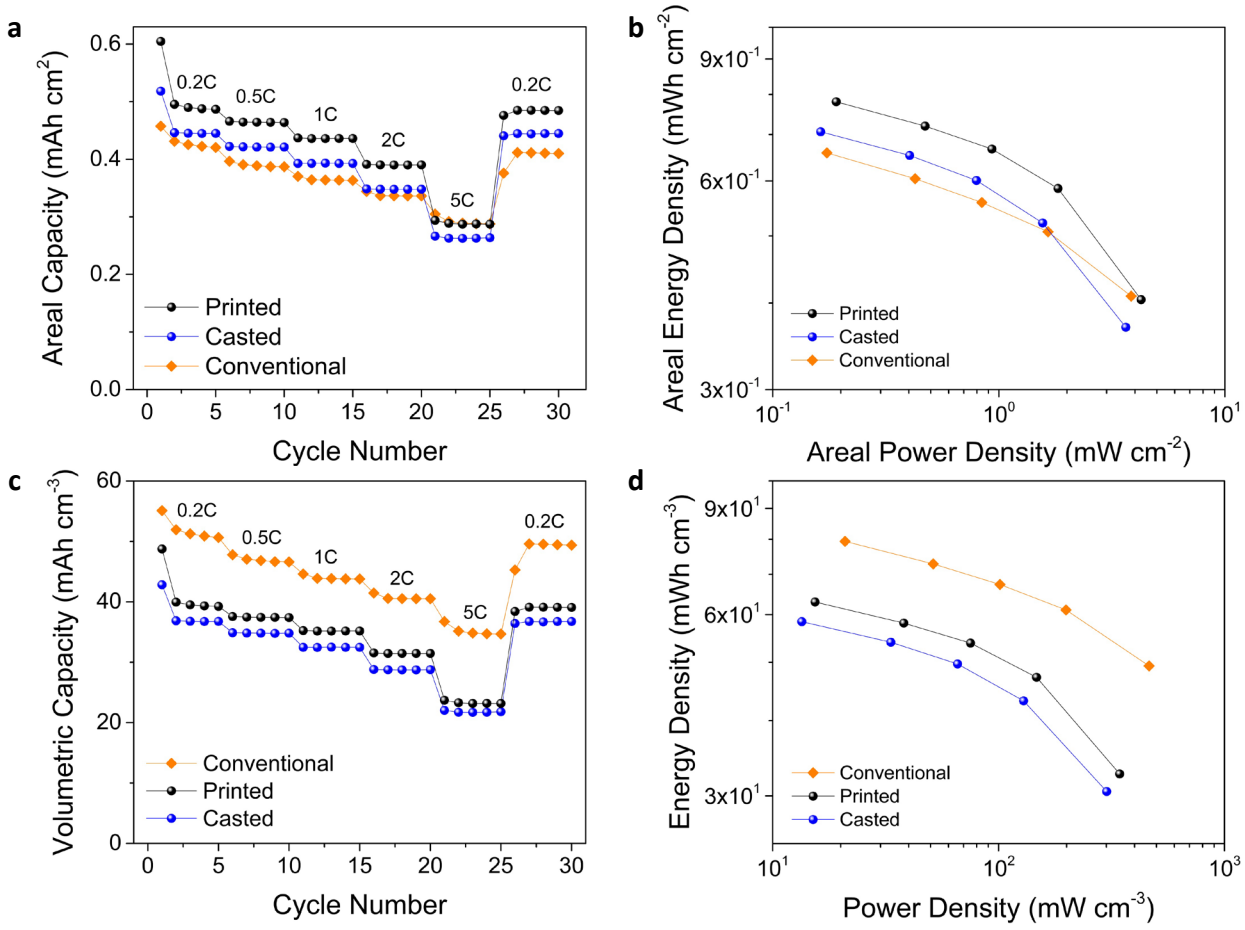


**Fig. S9.** Comparison of electrochemical properties of casted and printed composites (sample B) and a conventional $Li_4Ti_5O_{12}$ electrode on copper foil (70:20:10 $Li_4Ti_5O_{12}$:graphite:PVDF). All three samples contain between 3.0-3.5 mg cm$^{-2}$ active loading.

**References**

[1] A. J. Bard, L. R. Faulkner, *Electrochemical Methods: Fundamentals and Applications*, Wiley, New York **2001**.